

Review

Orientation of Chiral Molecules by External Electric Fields: Focus on Photodissociation Dynamics

Po-Yu Tsai ¹ and Federico Palazzetti ^{2,*} ¹ Department of Chemistry, National Chung Hsing University, Taichung 402, Taiwan² Dipartimento di Chimica, Biologia e Biotecnologie, Università degli Studi di Perugia, Via Elce di Sotto 8, 06123 Perugia, Italy

* Correspondence: federicopalazzetti@yahoo.it

Abstract: Molecular orientation is a fundamental requirement to study and control photoinitiated reactions. Experimental setups that make use of hexapolar electric filters combined with slice-ion imaging detectors were employed in these last years to investigate the photodissociation dynamics of chiral molecules. The final goal is the on-the-fly discrimination of oriented enantiomers, revealed by the different angular distributions in photofragment ion-imaging, as predicted from vector correlation studies. Here, we review experiments of photodissociation of oriented chiral molecules, with the aim of presenting limits emerging from these investigations and perspectives toward the achievement of the ultimate objective.

Keywords: enantiomers; hexapole; chiral discrimination

1. Introduction

Molecular beam techniques have experienced significant developments since their introduction in the study of elementary chemical processes. This development was aimed at acquiring the control of translational, rotational, and internal degrees of freedom of the involved molecular species [1]. The first important achievement concerned the control of velocity and directionality of molecular beams, through the development of the time-of-flight mass-spectrometry [2] and the velocity selection [3], permitting investigation of single-collision processes (see for example [4,5]).

The introduction of ion imaging and laser techniques permitted setting up experiments with control of the internal degrees of freedom [6]. Likewise, techniques making use of electric and magnetic fields were developed to align and/or orient molecules. Alignment and orientation are two properties related to the spatial arrangement of molecules. They consist in the polarization of the total angular momentum: in the alignment the polarization is limited to the direction, whereas in the orientation both the direction and the sense of the total angular momentum vector are controlled. Orientation is a fundamental requirement in stereodynamics, since it permits eliminating the random rotation of the molecule, which inevitably conceals the geometry and symmetry properties of the system [7–9]. In photoinitiated processes, the angular distribution of fragments obtained by photodissociation of oriented parent molecules provides insights into the photodynamics processes. Methyl iodide, CH₃I, was the first oriented molecule to be investigated by imaging techniques [10]. A milestone, in these applications, was placed by Rakitzis et al. that elucidated the conditions that permit obtaining additional dynamical information in their study of the photodissociation of OCS [11].

Here, we review the state-of-art of the studies that make use of orientation and imaging techniques aimed at providing dynamical insights in photodissociation of chiral molecules [12]. Basically, in collisions involving two chiral encounters, the enantiomers are expected to be scattered differently, depending on the pair of involved enantiomers R-S or R-R, or equivalently S-R or S-S, where R and S denote the two mirror forms. The



Citation: Tsai, P.-Y.; Palazzetti, F. Orientation of Chiral Molecules by External Electric Fields: Focus on Photodissociation Dynamics. *Symmetry* **2022**, *14*, 2152. <https://doi.org/10.3390/sym14102152>

Academic Editor: Mateo Alajarin

Received: 5 September 2022

Accepted: 7 October 2022

Published: 14 October 2022

Publisher's Note: MDPI stays neutral with regard to jurisdictional claims in published maps and institutional affiliations.



Copyright: © 2022 by the authors. Licensee MDPI, Basel, Switzerland. This article is an open access article distributed under the terms and conditions of the Creative Commons Attribution (CC BY) license (<https://creativecommons.org/licenses/by/4.0/>).

enantiomers can be distinguished even if only one of the two encounters is chiral. The condition is that the encounters define three non-coplanar vectors, so that the whole system is still chiral. In this regard, theoretical models have been developed for elastic collision involving the electron-chiral molecule [13] and the rare gas atom-chiral molecule [14] and for reactive collision involving non-chiral-chiral molecule [15].

Molecular orientation is realized by electrostatic hexapoles with DC (Direct Current) electric fields. A hexapole is a device composed of six metal bars arranged according to a hexagon along the molecular beam expansion axis, with a length that is commonly between 50 cm and 2 m. A voltage is applied to the bars, generating an inhomogeneous electric field, which is 0 along the hexapole axis and increases by approaching the bars. Electrostatic hexapole field were initially used to select rotational states in linear [16] and symmetric-top molecules [17] and as electrostatic lenses to focus molecular beams [18]. After 2000, it has also been applied to asymmetric-top molecules [19], opening the way toward the application to the more complex chiral molecules [20–22], where rotational-state manifolds are too dense to permit an efficient rotational state-selection [23]. Hexapoles have been combined with other techniques to orient molecules for collision and photodissociation experiments. For this goal, scattering experiments have been performed by orienting molecules with hexapoles and D.C. electric fields, which is the main topic of this review. Here, we review photodissociation studies on the chiral molecules 2-bromobutane [24–26], 1-bromo-2-methylbutane [27], and (R)-3-bromocamphore [28], and also review the photodissociation of non-oriented halothane [29].

We conclude this introduction by mentioning some other orientation techniques that make use of external electric fields to spatially separate enantiomers. Efrati and Irvine [30] provided measurements of the chirality based on the orientation, extending the original definition of Lord Kelvin. They demonstrated that the mirror form of a single object can be simultaneously left-handed or right-handed when it is considered from different directions. Shang et al. [31] studied the effect of orientation ordering induced by domains in the structure of C₆₀ thin films grown on Cd surfaces. Gershnel and Averbukh [32] investigated chiral molecules by a pair of laser fields with twisted polarization; the excitation produced by this set up induces a torque directed along a defined axis, resulting in a transient molecular orientation. They observed that enantiomer pairs are oriented in opposite directions. A. Milner et al. [33] performed experimental demonstration of rotational control of the two enantiomers of the chiral molecule propylene oxide by means of an optical centrifuge. An approach based on an optical centrifuge combined with a static electric field that produces a chiral field, allowing spatial separation of enantiomers was presented by Yachmanev et al. [34]. Finally, the experiment performed by T.-M. Su is worthy of note. He employed a screw pumping system to produce enantiomer enrichment in the gas phase of the chiral rotamer CH₃-CHClBr, according to the rotation direction of the pumps [35,36].

2. Background

In this review, we consider photodissociation experiments involving chiral molecules and linearly polarized lasers. In linearly polarized light, the electric field vector (or the magnetic field vector) is confined to a certain plane along the direction of propagation. For circularly polarized light, the electric field is formed by two linear components that are perpendicular to each other, equal in amplitude, but with a phase difference of $\pi/2$. The resulting electric field rotates in a circle around the direction of propagation. Depending on the rotation direction, the circularly polarized light is called right-handed or left-handed.

2.1. Molecular Alignment and Orientation

In the research area of chemical reaction dynamics, the “polarization” of a vector property implies a situation where the spatial distribution of such a property is not isotropic. One often uses the terms alignment and orientation to characterize polarizations of the rotational angular momentum of molecules. This concept can be defined by describing the

spatial distribution of an ensemble of single-headed arrows (vectors) [37,38]. If the spatial distribution of the arrows ensemble shows a preference, by pointing toward a certain direction along a given axis (e.g., the direction $+Z$ along an axis Z), such a preference is called orientation of the (arrow) vector ensemble. If there is no preference in the direction of the arrows, i.e., the arrows are parallel to the Z -axis, but half of them point toward $+Z$ and the remaining half point toward $-Z$, the vector ensemble is no longer oriented. However, there is still a polarization of the vector ensemble since the vectors are parallel to the Z -axis. Such a preference, where the arrows are equivalently parallel or antiparallel to the Z -axis is called the alignment of the vector ensemble.

Considering the vector ensemble constituted by angular momentum vectors \mathbf{J} , if the directional distribution of \mathbf{J} is cylindrical symmetric with respect to the Z -axis, the orientation and alignment can be represented by multiple expansion of the Legendre polynomial moments in terms of $\cos(\theta)$, where θ is the polar angle between \mathbf{J} and Z . In a such framework, the monopole term is proportional to the population. All the odd multipoles (dipole, octupole, etc.) describe the orientation of \mathbf{J} , while all the even multipoles (quadruple, hexadecapole, etc.) are related to the alignment of \mathbf{J} . When all the orientation and alignment multiple terms vanish in the expansion, the spatial distribution of \mathbf{J} is isotropic, and the vectors are uniformly distributed in space.

2.2. Experimental Set-Up

In Figure 1, we report the scheme of a typical experimental setup consisting of a molecular beam apparatus combined with a hexapole field, ion-optics for both molecule-orientation and ion-extraction, one or two tunable nanosecond-pulse laser beams for photolysis and resonance enhanced multiphoton ionization (REMPI) combined with slice-ion imaging technique for state-resolved photofragment velocity detection [39–41]. The vacuum system is composed of three chambers, separated by differential pumping, where the molecular-beam source, the hexapole selector, and the imaging detector system are accommodated. After passing through a skimmer and a collimator, the skimmed molecular beam enters a chamber equipped with the hexapole state selector, where molecules with specific rotational states can be focused at a given hexapole voltage. The selected molecules finally reach the ion photofragment imaging system, where these molecules, aligned by hexapole, are oriented, photodissociated and detected.

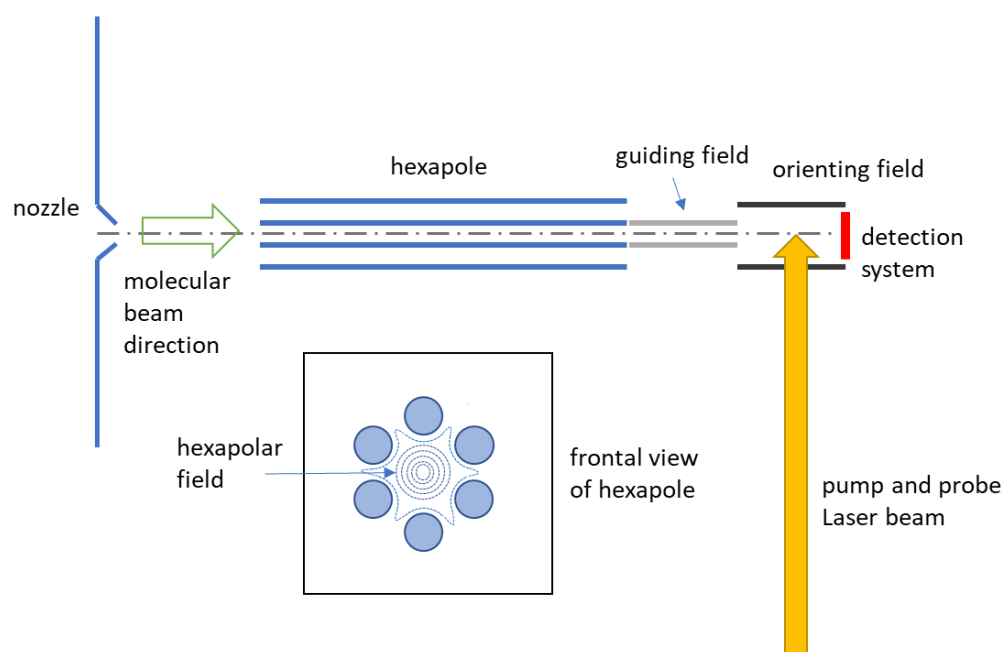


Figure 1. Schematic view of a typical molecular beam apparatus combined with a hexapole (two of the six bars are eclipsed) and a single laser.

2.3. Alignment and Orientation Induced by Electric Fields

The hexapole state selector is composed by six metal rods, in the frontal view they are arranged in hexagon along the molecular beam axis. Hexapole produces a non-uniform electric field, which is zero along its axis (coincident with the beam propagation axis) and increases by approaching the rods. Its effect is to select rotational states, align molecules and focus molecular beams. In the case of the photodissociation of OCS [11], they could select a single rotational quantum state that, in absence of nuclear spin, could be conserved until reaching the orienting field. Chiral molecules are generally heavier and more complex than OCS, thus selection of single rotation states is not possible.

Molecular alignment is achieved with the aid of hexapoles in supersonic beam conditions. Molecules with angular momentum vectors oriented in certain directions of the space can be selected and focused by hexapolar fields to achieve “angular momentum alignment”. Molecular orientation is obtained by applying static electric DC fields on pre-aligned molecules. Molecules in different rotational states possess different directional properties of their angular momentum, including the angular momentum projection on the principal axes of molecular frame. Thus, selecting molecules with certain rotational states, one equivalently generates an ensemble of molecules with their principal axes distributed anisotropically in the laboratory frame. In other words, one can generate molecules with their principal axes oriented or aligned in the laboratory frame coordinates, in order to achieve “molecular orientation” or “molecular alignment”, respectively. The molecular orientation and alignment are defined with respect to a quantization axis that corresponds to the direction of the electric field. It is typically denoted as Z-axis of the laboratory reference frame.

If an internal molecular rovibronic state (φ) is represented as a linear combination of a certain complete basis set functions, the expectation value of the molecular orientation and alignment can be calculated quantitatively by evaluating the corresponding Legendre moments of odd orders and even orders with respect to the Z-axis, $\langle \varphi | P_l(\cos \theta) | \varphi \rangle$, respectively, where $P_l(\cos \theta)$ is the l -th order Legendre polynomial and θ denotes the polar angle with respect to the Z-axis. If one requires the detailed orientational properties, beyond these expectation values of Legendre moments, the orientational probability distribution function (OPDF), calculated by the square modulus of the state function φ in position representation, could provide further information.

For a symmetric-top molecule in a field-free rotational state (J, K, M), its OPDF is expressed in terms of orthogonal expansion of Legendre functions:

$$P_{JKM}(\cos \theta) = \sum_{n=0}^{2J} \langle P_n(\cos \theta) \rangle P_n(\cos \theta) = \frac{2J+1}{2} \sum_{n=0}^{2J} c_n P_n(\cos \theta),$$

where the c_n coefficients denote the Legendre moments divided by a common factor $(2J+1)/2$. The Legendre moments can be expressed in terms of the Wigner 3-j symbols:

$$\langle P_n(\cos \theta) \rangle = \langle \varphi_{JKM} | P_n(\cos \theta) | \varphi_{JKM} \rangle = \frac{2J+1}{2} (-1)^{M-K} (2n+1) \begin{pmatrix} J & J & n \\ K & -K & 0 \end{pmatrix} \begin{pmatrix} J & J & n \\ M & -M & 0 \end{pmatrix}$$

The meaning of the sign of the Legendre moments (or the expansion coefficients, c_n) can be understood as follows. Consider the first Legendre moment, which is just $\langle \cos \theta \rangle$. The negative value means that the angle θ is $>90^\circ$, thus the sign of the first Legendre moment (or c_1) can be explained as the relative direction of the average orientation with respect to +Z direction. Similarly, the sign of the second Legendre moment (or c_2) can be interpreted as the axis of the average alignment that tends to be parallel (positive sign of c_n) or perpendicular (negative sign of c_n) with respect to the Z-axis.

It is noteworthy that the OPDF of the molecule should be positive for any value of θ , therefore the values of the c_n coefficients are always bounded to fulfill this constraint. Consider a non-uniform molecular OPDF with the expansion that can be truncated up to c_2 term (first alignment moment), then it is improbable that such OPDF possesses large c_1 , except with $c_0 = c_2 = 0$. In such a case, the OPDF may possess negative value somewhere

(due to $P_1(\cos\theta)$) and becomes entirely unrealistic. In other words, a highly oriented molecular distribution usually possesses non-negligible alignment moment in their OPDF. On the contrary, a purely aligned molecular distribution could be realistic even without any odd-order terms in OPDF.

The rotational states of asymmetric top molecules are characterized by a pseudo quantum number (τ) instead of the good quantum number K . In field-free conditions, their OPDF can be expressed as:

$$P_{J\tau M}(\cos\theta) = \sum_{K'K''} \delta_{K'K''} a_{K'}^{J\tau} a_{K''}^{J\tau} \frac{2J+1}{2} (-1)^{M-K''} \sum_{n=0}^{2J} (2n+1) \begin{pmatrix} J & J & n \\ K' & -K'' & 0 \end{pmatrix} \begin{pmatrix} J & J & n \\ M & -M & 0 \end{pmatrix} P_n(\cos\theta),$$

where $a_{K'}^{J\tau}$ or $a_{K''}^{J\tau}$ are the expansion coefficients of field-free asymmetric-top rotational states expanded on symmetric-top functions. The quantum numbers with superscript prime or double-prime characterize the mixed symmetric-top states. The situation is even more complicate in presence of an electric field. Levels with a different quantum number J could be mixed by the electric field. It turns out that the only good quantum number remained to characterize the rotational state of asymmetric top molecules is the laboratory frame projection quantum number, M . The OPDF of asymmetric-top rotational states is in general field-dependent when represented in terms of symmetric-top basis:

$$P_{J\tau M}(\cos\theta, \varepsilon) = \sum_{J'J'' \tau'\tau'' K'K''} \delta_{K'K''} c_{J'\tau'}^{J\tau M}(\varepsilon) c_{J''\tau''}^{J\tau M}(\varepsilon) a_{K'}^{J'\tau'} a_{K''}^{J''\tau''} \frac{(2J'+1)^{1/2} (2J''+1)^{1/2}}{2} (-1)^{M-K''} \sum_{n=|J'-J''|}^{J'+J''} (2n+1) \begin{pmatrix} J' & J'' & n \\ K' & -K'' & 0 \end{pmatrix} \begin{pmatrix} J' & J'' & n \\ M & -M & 0 \end{pmatrix} P_n(\cos\theta),$$

with the field-dependent expansion coefficients $c_{J'\tau'}^{J\tau M}(\varepsilon)$ and $c_{J''\tau''}^{J\tau M}(\varepsilon)$ that are originated from the coupling between states with different J numbers due to the Stark interaction.

2.4. Photofragment Ion-Imaging

The state-selected molecules enter the photofragment ion-imaging system through the ion lenses, which are placed downstream from the hexapole exit. Prior to intersect with the polarized photolysis laser beam inside the first stage of the ion lenses, consisting of four plates, the molecules are oriented by electrostatic homogeneous field to have the permanent dipole pointing toward or backward along the direction of the TOF axis, the molecule is thus oriented. If the backward orientation is required, the orienting field provided by ion-lenses can just be reversed by adjusting the electric voltage of individual plate of ion-lenses. After achieving the photolysis of the oriented molecular ensemble, the extraction plate of the ion lenses can be switched to the ion extraction field for ion-imaging detection. The photofragment ions are generated by a second tunable ns-pulse laser (denoted as "probe" laser) to ionize the neutral fragment via REMPI technique. The resulting ions are extracted and accelerated into a field-free drift tube along the molecular beam direction. The ion-cloud expansion is mapped onto a two-stage microchannel plate (MCP) coupled with a phosphor screen. Then, ion imaging on the phosphor screen is recorded by a charge-coupled device (CCD) camera. The gate pulse of the MCP can be controlled to perform two types of image data acquisition: either to apply a wide gate (the order of 500 ns) to cover the whole three-dimension ion cloud, map the ion-cloud onto the two-dimension detector plane (velocity-mapping image), or to apply a narrow gate (the order of 25 ns) to acquire a portion of the whole ion cloud along TOF axis (slice-ion image). The acquired ion-image data, either the velocity-mapping [39] or sliced image, is expressed as a function of two-dimension plane (of MCP detector). Each image contains information about the magnitude and direction of the photofragment velocity vectors, providing that all the signals on an image are from fragments of the same mass and arrival time. The position of signals on the image only depends on the velocity components which is perpendicular to the TOF axis (i.e., the transverse velocity component), therefore when the position corresponding to zero transverse velocity of the photofragment is located and serves as the

origin of the image, the relative position of any point from that origin could be represented in polar coordinates (r, θ) . It is obvious that r is proportional to the magnitude of velocity vector, while θ provides information about the angular distribution of the photofragment, with respect to the projection of the polarization vector of photolysis laser on MCP plane. Analysis of the velocity in ion image data can provide information about the geometrical and dynamical effects of a molecular photodissociation process.

2.5. The Semiclassical Vector Model

Herein, we present the correlation between some dynamical vector properties that lead to the discrimination of molecular chirality by linearly polarized laser light. In Figure 2, we consider the vector properties of a polyatomic molecule, where a semiclassical vector scheme in the electric dipole approximation of light-matter interaction is assumed. The vectors we consider are the permanent electric dipole, \mathbf{d} , of the molecule on the equilibrium geometry of the electronic ground state surface, the transition dipole moment (of electronic ground and excited states), $\boldsymbol{\mu}$, and the recoil velocity, \mathbf{v} , of the photofragment, which is generated after electronic excitation of molecule. These three vectors are defined in the molecular recoil frame (xyz) , where the z -axis is defined by the direction of \mathbf{v} . We also define the polar angles α ($0 \leq \alpha \leq \pi$) and χ ($0 \leq \chi \leq \pi$), given by the intersection between \mathbf{v} and \mathbf{d} , and \mathbf{v} and $\boldsymbol{\mu}$, and the azimuthal angle, ψ ($0 \leq \psi \leq 2\pi$), given by the intersection of the x -axis and the projection of $\boldsymbol{\mu}$ onto the xy -plane. For chiral molecules involved in photodissociation experiments, the sign of ψ is characteristic of the enantiomers and can be determined by photofragment angular distribution of the oriented chiral molecule. In other words, distinct mirror forms are related to $+\psi$ or $-\psi$, while for achiral molecules this correspondence is not univocal. Rakitzis et al. reported the relation between molecular frame information and experimental observables [12]. For a given XYZ laboratory frame coordinates, Z corresponds to the molecular beam axis, while Y is the direction of the laser beam propagation. The two beams intersect each other at the center of the ion optics system and the XY -plane includes the detected photofragments, where velocities and angular distributions are measured. In slice-ion imaging the angles α , χ and ψ are determined from specific directions of the light polarization and orienting field [38,39]. To derive the general equation of slice-image intensity, one starts from predicting the intensity formula by investigating the relation among \mathbf{v} , \mathbf{d} , $\boldsymbol{\mu}$, orienting field axis, and photolysis laser polarization in molecular frame coordinates (Figure 3). Then, one performs the coordinate transformation from molecular frame to laboratory frame, obtaining the image intensity formula as a function of the azimuthal angle on the XY -plane in the laboratory frame. Here, we shall not discuss the general formulae, since the total number of variables is too high to be investigated simultaneously in practical applications. On the contrary, we present two special arrangements that are capable of providing physical insights about the directional properties about transition dipole, permanent dipole, molecular chirality, and OPDF.

A first experimental arrangement is made by an orienting electric field, whose vector is applied along the $+Z$ direction (toward the detector). The polarization vector of the linearly-polarized light (for photolysis) possesses a polar angle of 45° with respect to the X -axis. Besides, we assume that the OPDF of the molecule can be characterized by truncating the expansion of Legendre polynomials up to the second order Legendre moment (c_2). With such a special setting, the angular dependent intensity of a slice image can be expressed in terms of the laboratory frame coordinates, providing that the electric dipole approximation is hold for a one-photon photolysis process:

$$I(\theta) \propto \sum_{l=0}^2 \sum_{m=0}^1 \frac{b_l^m}{b_0^0} P_l^m(\cos \theta) = 1 + \beta_1^0 P_1^0(\cos \theta) + \beta_2^0 P_2^0(\cos \theta) + \beta_1^1 P_1^1(\cos \theta) + \beta_2^1 P_2^1(\cos \theta),$$

where $P_l^m(\cos \theta)$ are the associated Legendre function and β_l^m the corresponding expansion coefficients. The directional properties of the vector quantities in the molecular frame can be extracted from the expansion coefficient β_l^m by using the following formulae:

$$\begin{aligned}\beta_0^0 &= (1 - c_2 P_2(\cos \alpha)) \left(1 - \frac{1}{2} P_2(\cos \chi)\right) + \frac{3}{16} c_2 \sin^2 \alpha \sin^2 \chi \cos 2\psi \\ \beta_1^0 &= 3c_1 \sin \alpha \sin \chi \cos \chi \cos 2\psi \\ \beta_2^0 &= (1 - c_2 P_2(\cos \alpha)) P_2(\cos \chi) + \frac{3}{8} c_2 \sin^2 \alpha \sin^2 \chi \cos 2\psi \\ \beta_1^1 &= -\frac{9}{8} c_2 \sin^2 \alpha \sin^2 \chi \sin 2\psi \\ \beta_2^1 &= -c_1 \sin \alpha \sin \chi \cos \chi \sin 2\psi\end{aligned}$$

where the coefficients c_1 and c_2 come from the leading terms of OPDF (Equation (1)) expanded by the Legendre polynomials. If the molecules are not oriented or aligned, $c_1 = c_2 = 0$, then the above formula can be reduced to the well-known angular distribution equation of randomly oriented molecules:

$$I(\theta) \propto 1 + \beta_2^0 P_2(\cos \theta) \quad \beta_2^0 = 2P_2(\cos \chi)$$

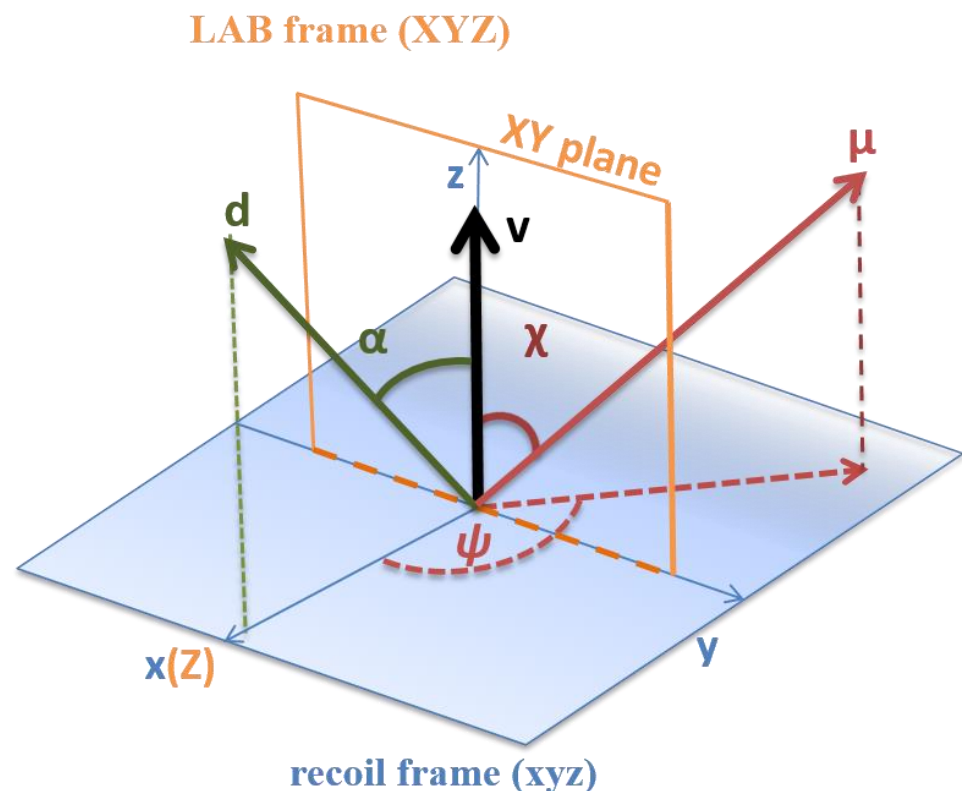


Figure 2. Vectors \mathbf{d} , \mathbf{v} , $\boldsymbol{\mu}$ and the angles α , χ , and ψ in the recoil frame xyz and in the laboratory frame XYZ .

Terms β_l^{l-1} contribute to the up-down asymmetry of slice images. Recalling that the orienting field vector is perpendicular to the detector plane XY , the up-down asymmetry in slice images should be attributed to the relative orientation of \mathbf{d} and $\boldsymbol{\mu}$ vectors. Besides, the left right asymmetry of image may arise from the terms with coefficients containing $\sin 2\psi$, providing that ψ is neither 0° nor 180° . Such left-right asymmetry can lead to a tilted image pattern, which is the key feature required for the chiral discrimination by this technique. The geometric explanation to this asymmetry feature is that if the three vectors ($\boldsymbol{\mu}$, \mathbf{d} and \mathbf{v}) are coplanar (i.e., $\psi = 0^\circ$ or 180°), then the chirality could not be characterized by these vectors.

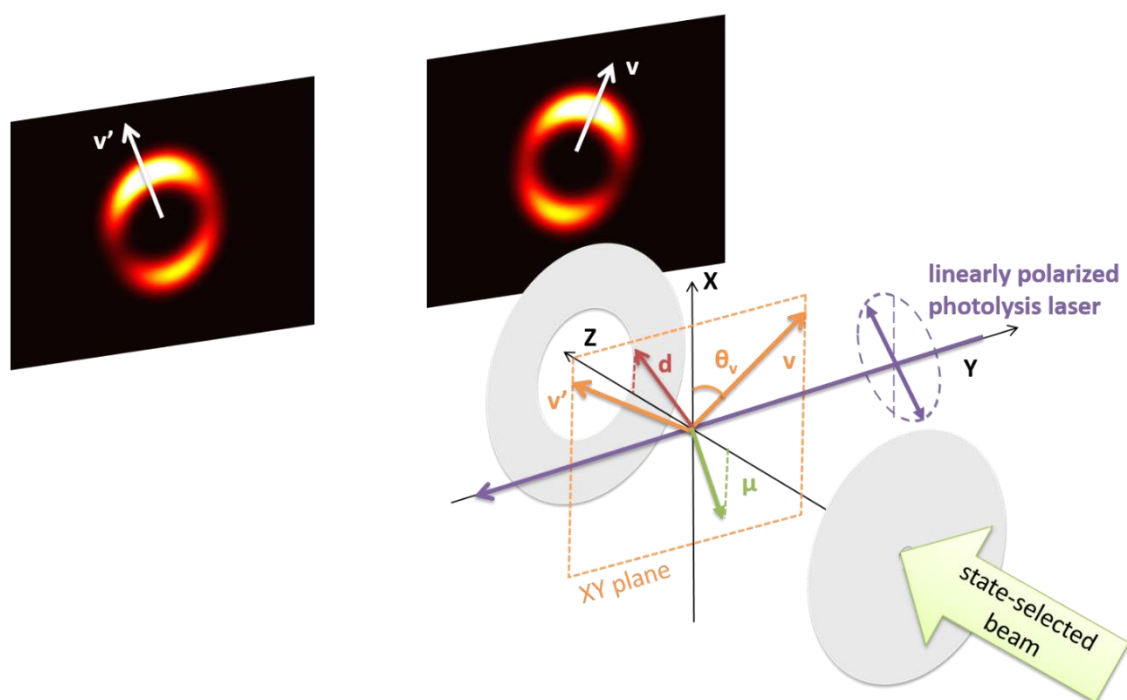


Figure 3. The semiclassical vector scheme in the electric dipole approximation of linearly polarized photolysis laser (the polarization plane is indicated by the violet arrows) interacting with a hypothetical polyatomic molecule in a state-selected beam, where the vectors recoil velocity \mathbf{v} , permanent electric dipole moment \mathbf{d} , and transition dipole moment $\boldsymbol{\mu}$ are defined. Enantiomer pairs are dissociated with different directions of the recoil velocities, \mathbf{v} and \mathbf{v}' . The corresponding photofragment ion images, here depicted, present tilted and specular angular distributions given by the photodissociation of an enantiomer pair.

The second experimental arrangement can be adopted when the polar angle between \mathbf{d} and $\boldsymbol{\mu}$, denoted as $\theta_{\mu d}$, must be determined. The experimental arrangement is the same as the first except that the polarization of the photolysis laser that in this case is variable. This setting allows one to investigate the so-called vector correlation between laser light polarization and permanent dipole moment (\mathbf{d}). Such a vector correlation could be attributed to the relative direction of \mathbf{d} and $\boldsymbol{\mu}$ vectors. The corresponding formula of image intensity is obtained by integrating over the direction of \mathbf{d} vector as well as azimuthal angle (θ) in laboratory frame. The result is the function of a polar angle (Γ) which characterizes the polarization vector of linearly polarized light with respect to the X-axis:

$$I(\Gamma) \propto 1 + \beta' P_2(\cos \Gamma), \quad \beta' \equiv \frac{4}{5} c_2 P_2(\cos \theta_{\mu d})$$

Important features could be extracted from the above formula, where β' serves as the origin of the laser polarization dependence of image intensity. If \mathbf{d} and $\boldsymbol{\mu}$ vectors are orthogonal in the molecular frame, then there would be no polarization dependence in the intensity, since $\beta' = 0$. Besides, the molecular ensemble must possess non-zero Legendre moment of even-order (c_2 , alignment). In other words, it is impossible to investigate such a vector correlation for a randomly-oriented molecular distribution ($c_2 = 0$), no matter how the \mathbf{d} and $\boldsymbol{\mu}$ vectors are placed in molecular frame. It is worth emphasizing that the polarization dependence formula is independent on the odd-order Legendre moment (e.g., c_1) in OPDF, thus the measurement can work with an aligned molecular distribution. Lacking c_1 coefficient in the above formula could be understood by recalling that the light polarization serves as a “double-headed arrow” when considering the transition probability in electric dipole approximation, thus it raises the same electronic transition probability (for

the signal intensity is proportional to its modulus square) for a molecule either oriented in one direction or the opposite direction at a given Γ angle.

3. Review of Photodissociation Experiments on Oriented Chiral Molecules

In this section, we describe the methodology and report the main results on photodissociation experiments carried out on chiral molecules oriented by making use of the electrostatic hexapole technique.

3.1. Photodissociation of Oriented 2-Bromobutane

2-bromobutane (Figure 4) is a chiral molecule characterized by three conformers, T, G+ and G−, that show a similar beam intensity vs. hexapole voltage dependence. A pure supersonic beam has been aligned and rotationally selected by a 70 cm-length hexapole, with a radius of 4 mm.

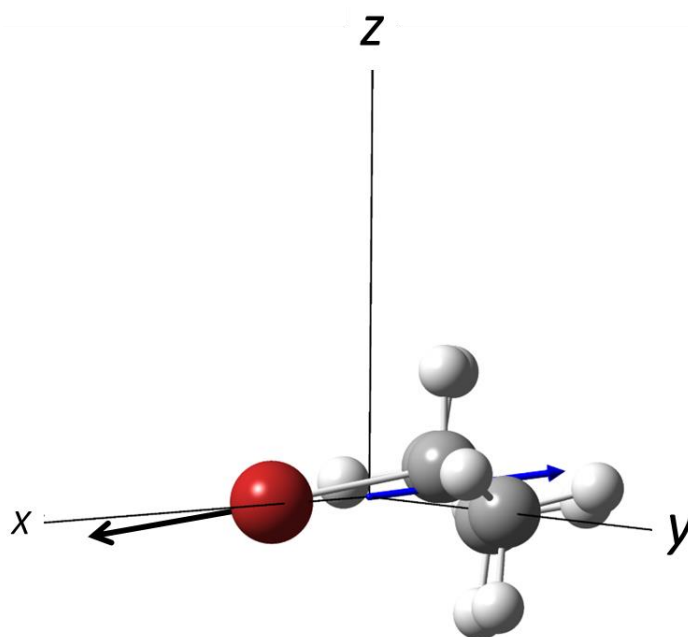


Figure 4. The structure of 2-bromobutane, in red the Br atom, in grey the C atoms, and in white the hydrogens. The permanent dipole moment direction is indicated by the blue arrow, the recoil velocity vector (in black) is parallel to the C–Br bond according to the recoil axis approximation.

The experimental setup consists of three chambers, separated by differential pumping, containing the molecular beams source, the electrostatic hexapole and a slice-ion imaging detector system (further details are given in Ref. [24]). The hexapole extremity is placed 2 cm far from the entrance of the ion lenses, which are part of the ion-imaging system and generate an extraction field of 200 V/cm that plays a double role: (i) it orients the previously aligned molecules, (ii) it accelerates the photofragments to the detector. This small distance guarantees the adiabatic passage of the molecules from the hexapole field to the extraction field, without losing the alignment. A one-color laser has been produced to emit at ca. 234 nm with 400 μ J per pulse. The polarization direction of the laser beam is perpendicular to the molecular beam axis and parallel to the imaging surface. This single laser beam has been employed to photodissociate the 2-bromobutane molecule and to probe, by (2 + 1) resonance-enhanced multiphoton ionization (REMPI) technique, the Br fragment both in the ground ($^2P_{3/2}$) and excited state ($^2P_{1/2}$), at 233.7 and 234.0 nm, respectively. This photodissociation process involves a single electronic state. The anisotropy parameters determined from the experiment are $\beta = 1.49$ for Br ($^2P_{3/2}$) and $\beta = 1.85$ for Br ($^2P_{1/2}$).

Molecular orientation is verified by means of time-of-flight measurements, considering that (1) forward-recoiled photodissociated bromine reaches the detector directly, while

(2) the backward-recoiled bromine photofragment is first directed to the repeller plate and then accelerated by the extraction field. In such a way, (2) reaches the detector later than (1). For non-oriented molecules, fast and slow fragments are equally distributed, such a behavior is revealed by two peaks of similar intensity. On the contrary, in case of oriented molecules, the peaks display different intensities (see Figure 4 in Ref. [24]).

As introduced previously, the ion lenses produce a weak electric field, ca. 200 V/cm, that permits both the extraction and the molecular orientation. To control molecular orientation, a pulsed voltage (with a very short response time of 30 ns) was applied at the ion extraction stage, permitting to modulate both the intensity and the sense of the orienting field vector. Separation of the ion extraction and molecular orientation stages allows one to use a strong electric field to orient molecules of a very high complexity, while maintaining a weak electric field for the ion extraction. It opens important perspectives in view of future applications.

A subsequent study was performed to investigate photodissociation processes involving multiple electronic states [25]. At 238 and 254.1 nm, the excitation of 2-bromobutane that determines the bond breaking of the C–Br bond involves the excited states 3Q_1 , 3Q_0 and 1Q_1 , where 3Q_1 and 1Q_1 are perpendicular transitions with respect to the C–Br bond axis and correlates to $Br(^2P^0_{3/2})$. The electronic state 3Q_1 is instead a parallel transition, with respect to the C–Br bond axis, and correlates to $Br(^2P^0_{1/2})$.

Photodissociation at 238.6 nm was investigated without hexapole field, and by applying hexapole voltage of 3 and 4 kV, to evaluate the top-bottom symmetry of the ion-imaging and the anisotropy parameter β . The β parameter has been estimated for the Br in the excited state, $Br(^2P_{1/2})$, and it turned to be very close to the parallel limit of 2, $\beta = 1.93$. It suggests that Br^* is photodissociated from a parallel transition, the electronic state 3Q_0 . In the presence of the electric field, produced by the hexapole voltage at 4.0 kV, the ion imaging presents a top-bottom asymmetry along the laser polarization axis. The best fitting, obtained by applying Equation (2) gave $\beta_1 = 0.67$ and $\beta_2 = 1.03$. This latter parameter is still typical of a parallel transition but smaller than that obtained without applying hexapole field. At HV = 3.0 kV, the ion imaging is still asymmetric, with $\beta_1 = 0.37$ and $\beta_2 = 1.04$. Evaluation of the asymmetry parameters indicate that while β_2 is almost unchanged with respect to the experiment at HV = 4.0 kV, β_1 is smaller, revealing a lower extent of the asymmetry. Such a difference was attributed to a different distribution of the rotational states of the aligned molecules.

The ion image at 254.1 nm of Br photofragment from non oriented molecule gives anisotropy parameter $\beta = 0.93$, typical of a perpendicular transition dissociation. At HV = 4 kV, the β_1 and β_2 asymmetry parameters are 0.24 and 0.12, that reveal a higher isotropic distribution of the photofragments, with a pronounced perpendicular transition originated from 3Q_1 combined with a strong non adiabatic coupling between 1Q_1 and 3Q_0 (Figure 1 in Ref. [25]).

For this molecule, the analysis of the selected rotational state permitted to determine which states are more enhanced under electrostatic hexapolar field. An interesting result is shown in Figure 3 of Ref. [25], where the population enhancement is plotted versus $M/J(J+1)$. The analysis revealed that high values of the hexapole voltage (4.0 kV) are capable to enhance the population of rotational states with $M/J(J+1) < 0.1$.

Three-vector correlation was carried out on the sliced ion images acquired at 234.0 and 254.1 nm [26]. The angles α and γ were determined from the experimental results, giving the following values: 164° and 163° , while the value of the angle between μ and d , also estimated from the experimental data, is 0° . These results show that it is not possible to distinguish between the two mirror forms, due to a planar configuration of the three vectors v , μ and d , being $\psi = 0^\circ$ and α and γ close to 180° (see Figures 2 and 6 in Ref. [26]). Additionally, for multi-potential photodissociation processes resulting from perpendicular transitions mixed with non-adiabatic ones, the recoil frame angles are not accurately evaluated.

3.2. Photodissociation of Oriented 1-Bromo-2-Methylbutane

The characterization of the photodissociation dynamics of 1-bromo-2-methylbutane (Figure 5) was performed by using both a single-laser and a two-laser experiment [27]. This latter setup permits to disengage the pump laser and the probe laser, allowing one to explore more dissociation pathways. This study represented a step forward toward the characterization of the photodissociation dynamics of more complex and more asymmetric molecules. The focusing curve showed an appreciable response of the dipole moment to the change of the hexapole field. Moreover, it was revealed to be suitable for molecular orientation with an average $\langle \cos \theta \rangle = 0.15$, where θ is the angle between the permanent dipole moment and the orienting field.

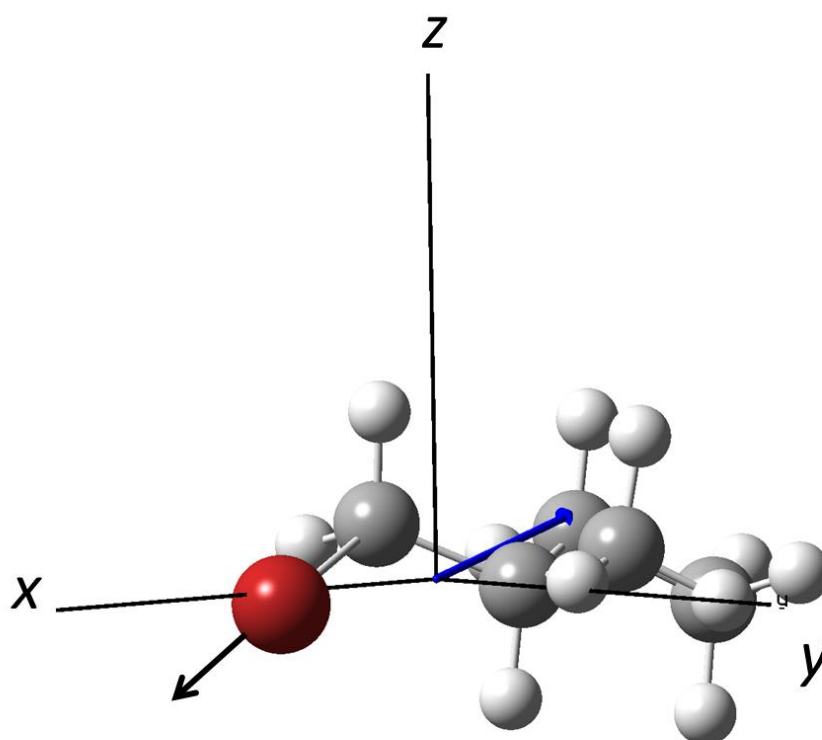


Figure 5. The structure of 1-bromo-2-methylbutane, in red the Br atom, in grey the C atoms, and in white the hydrogens. The permanent dipole moment direction is indicated by the blue arrow, the recoil velocity vector (in black) is parallel to the C–Br bond according to the recoil axis approximation.

One laser experiments were performed on non-oriented molecules at 232–233 nm. Ground state Br photofragments, $\text{Br}(^2\text{P}_{3/2})$, and excited state, $\text{Br}(^2\text{P}_{1/2})$, were ionized by $(2 + 1)$ REMPI and detected by slice-ion imaging. The image analysis gave the following values of the anisotropy parameter: $\beta = 1.88$ for the excited Br and $\beta = 0.63$ for the ground state Br. The first value denotes a parallel character of the transition that leads to the C–Br bond dissociation, while the second value reveals the involvement of photodissociation channels characterized by both perpendicular and parallel transitions. The angular analysis of the $\text{Br}(^2\text{P}_{1/2})$ photofragment distribution gave $\chi = 11.5^\circ$ and for α a value between 160° to 180° , while ψ was estimated 0° , similarly to what occurred for the photodissociation of 2-bromobutane.

The two-laser experiment permits to use probing lasers with different wavelength than that of the pumping laser. The authors probed the excited Br photofragment with a 240 nm wavelength laser, while the ground state Br was probed at 266.5 nm. The asymmetry parameters inferred from the imaging were 1.81 for $\text{Br}(^2\text{P}_{1/2})$ and 0.38 for Br, substantially confirming the results obtained with the single laser experiment, although the angular distribution of Br is more isotropic than that obtained at 232–233 nm. However, probing at 240 nm provides a better signal to noise ratio of the Br photofragment imaging.

3.3. Photodissociation of (R)-3-Bromocamphor at $\lambda = 234$ nm

Chang et al. investigated the photodynamics dissociation of 3-bromocamphor (Figure 6) by slice-ion imaging experiments on the bromine fragment at 234 nm [28]. They determined the anisotropy parameters for the bromine photofragments both in the ground state, Br ($^2P_{3/2}$), $\beta_1 = 0.75$, and in the excited state, Br ($^2P_{1/2}$), $\beta_1 = 0.48$. 3-bromocamphor is the heaviest molecule among those oriented by combining hexapole/orienting fields. The focusing curve shows a remarkable increasing of the signal, even at low values of hexapole voltage, confirming that focusing is a matter of symmetry, rather than molecular weight. The orientation distribution, $|\cos \theta_{do}|$, for this molecule is 0.35. Vector correlation analysis on dissociated Br ($^2P_{3/2}$) has shown that C–Br bond breaking is a rapid process, confirming that it was expected for this kind of experiment. For the Br ($^2P_{1/2}$) photofragment dissociated from a single parallel transition, which is dominant for this process, the angles χ , α , and ψ were estimated to 147° , 146° , and 0° , respectively.

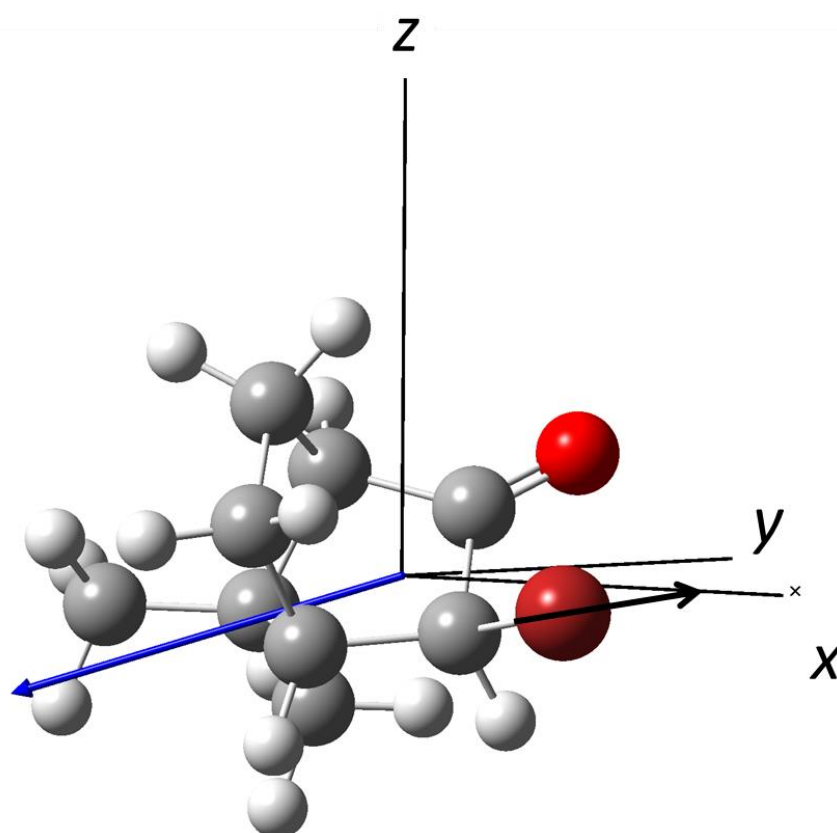


Figure 6. The structure of (R)-3-bromocamphor, in dark red the Br atom, in light red the oxygen, in grey the C atoms, and in white the hydrogens. The permanent dipole moment direction is indicated by the blue arrow, the recoil velocity vector (in black) is parallel to the C–Br bond according to the recoil axis approximation.

In addition, the isotropic angular distribution of the excited bromine photofragment depends on the contribution of the non-adiabatic transition from 1Q_1 to 3Q_0 , where perpendicular and parallel transitions are mixed.

3.4. Photodissociation of Halothane, CF_3CH_2Cl at $\lambda = 254.1$ nm

Photodissociation of the chiral molecules halothane ($CHClBr-CF_3$), in Figure 7, has been studied on non-oriented molecules at 234 nm, where both chlorine and bromine are dissociated from $n\sigma^*(C-Br)$ and $n\sigma^*(C-Cl)$ repulsive states [29]. Chlorine is dissociated also from a non-adiabatic interaction between the two surfaces. The branching ratio of chlorine versus bromine was measured, resulting 2:1. The set-up of this experiment consists

of a 1 m-hexapole which, acting both as electrostatic lens and filter, permitted obtaining intense beams, removing contaminations from clusters and excited conformers. Lack of orienting fields makes this experiment unable to detect possible chiral effects originating from photodissociation processes.

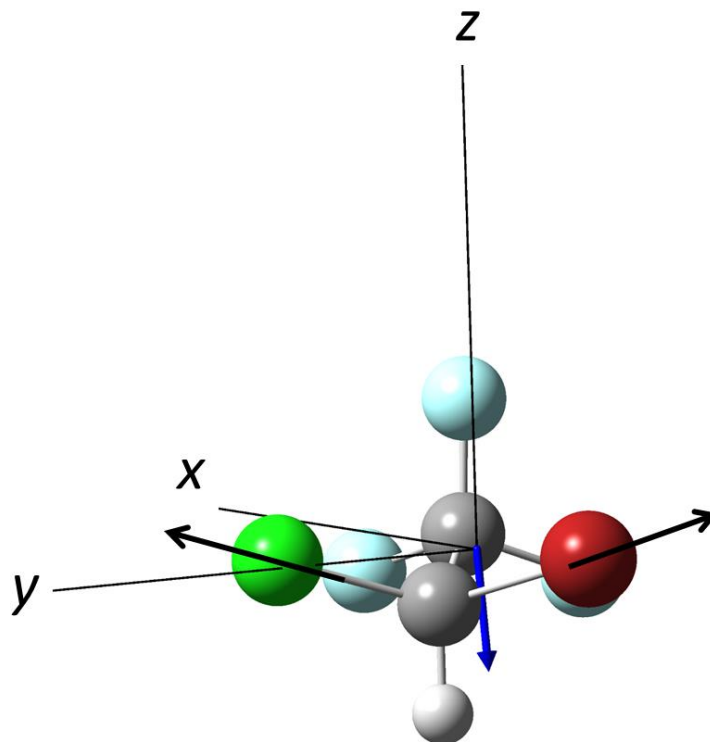


Figure 7. The structure of halothane, in red the Br atom, in green the Cl atom, in light blue the F atoms, in grey the C atoms, and in white the hydrogens. The permanent dipole moment direction is indicated by the blue arrow, the recoil velocity vectors (in black) are parallel to the C–Br bond and C–Cl bond according to the recoil axis approximation.

Very recently, Che et al. investigated the photodissociation dynamics of isohalothane, a non-chiral isomer of halothane [42]. Vector correlation analysis provided the main result of this work, which is the determination of the transition dipole moment for the specific case of asymmetric-top molecules (chiral molecules are a subclass of asymmetric-tops).

4. Final Remarks and Perspective

Various techniques that make use of a pair of external fields have been employed to spatially separate enantiomer pairs. Laser technique was applied by Gershnel and Averbukh, who made use of a pair of laser fields with twisted polarization, and by Milner et al., employing an optical centrifuge. Combination of an optical centrifuge and a static electric field was used by Yachmanev et al. We have also quoted the experiment of enantiomer enrichment performed by T.-M. Su, by using a screw pumping system.

In this review, we focused on the study of the photodissociation dynamics on molecules oriented by combining hexapole and D.C. static electric fields. The long road toward the main target of these studies—that is, the spatial separation of the enantiomers, which remains a challenge—permitted the arrangement of novel experimental setups, suitable to orient molecules with a low degree of symmetry. It has been observed that orientation depends essentially on molecular symmetry, instead of molecular mass. Photodissociations involving single-potential transitions are preferred to the multi-potential since the recoil frame angles are evaluated more accurately, as observed for 2-bromobutane. The use of a two-color laser scheme demonstrated an improvement in the signal to noise ratio.

The main obstacle toward the separation of enantiomers is due to the spatial arrangement of the three vectors that characterizes the dissociation process: permanent dipole moment, transition dipole moment, and recoil velocity. The separation is even more evident as the three vectors are far from the collinearity. For the molecules investigated so far, 2-bromobutane, 1-bromo-2-methylbutane, and 3-Br-camphor, the spatial separation cannot be detected. The strategy is that of moving in the direction of the search of a molecule with these characteristics. The next study must include a considerable theoretical effort that aims at predicting the excited electronic states related to transition dipole moments, which may ensure an appreciable spatial separation of the dissociated enantiomers.

Author Contributions: Conceptualization, P.-Y.T. and F.P.; methodology, P.-Y.T. and F.P.; software, P.-Y.T. and F.P.; validation, P.-Y.T. and F.P.; formal analysis, P.-Y.T. and F.P.; investigation, P.-Y.T. and F.P.; resources, P.-Y.T. and F.P.; data curation, P.-Y.T. and F.P.; writing—original draft preparation, P.-Y.T. and F.P.; writing—review and editing, P.-Y.T. and F.P.; visualization, P.-Y.T. and F.P.; supervision, P.-Y.T. and F.P.; project administration, P.-Y.T. and F.P.; funding acquisition, P.-Y.T. and F.P. All authors have read and agreed to the published version of the manuscript.

Funding: The research was funded by the Italian Ministry for Education, University and Research, MIUR, through SIR 2014 “Scientific Independence for Young Researchers” grant number RBSI14U3VF.

Institutional Review Board Statement: Not applicable.

Informed Consent Statement: Not applicable.

Data Availability Statement: Not applicable.

Acknowledgments: The authors are grateful to the late King-Chuen Lin, who made possible the realization of many experiments here reported.

Conflicts of Interest: The authors declare no conflict of interest.

References

1. Scoles, G. *Atomic and Molecular Beam Methods*; Oxford University Press: New York, NY, USA, 1988; ISBN 0195042808.
2. Boesl, U. Time-of-flight mass spectrometry: Introduction to the basics. *Mass Spectr. Rev.* **2017**, *36*, 86–109. [[CrossRef](#)]
3. Pirani, F.; Cappelletti, D.; Vecchiocattivi, F.; Vattuone, L.; Gerbi, A.; Rocca, M.; Valbusa, U. A simple and compact mechanical velocity selector of use to analyze/select molecular alignment in supersonic seeded beams. *Rev. Sci. Instrum.* **2004**, *75*, 349. [[CrossRef](#)]
4. Gilijamse, J.J.; Hoekstra, S.; van de Meerakker, S.Y.T.; Groenenboom, G.C.; Meijer, G. Near-Threshold Inelastic Collisions Using Molecular Beams with a Tunable Velocity. *Science* **2006**, *313*, 1617–1620. [[CrossRef](#)]
5. Van de Meerakker, S.Y.T.; Bethlem, H.L.; Meijer, G. Taming molecular beams. *Nat. Phys.* **2008**, *4*, 595–602. [[CrossRef](#)]
6. Suits, A.G. Invited Review Article: Photofragment imaging. *Rev. Sci. Instrum.* **2018**, *89*, 111101. [[CrossRef](#)]
7. Friedrich, B.; Herschbach, D.R. Spatial orientation of molecules in strong electric fields and evidence for pendular states. *Nature* **1991**, *353*, 412–414. [[CrossRef](#)]
8. Rakitzis, T.P.; van den Brom, A.J.; Janssen, M.H.M. Molecular and Laboratory Frame Photofragment Angular Distributions from Oriented and Aligned Molecules. *Chem. Phys. Lett.* **2003**, *372*, 187–194. [[CrossRef](#)]
9. Lipciuc, M.L.; van den Brom, A.J.; Dinu, L.; Janssen, M.H.M. Slice Imaging of Photodissociation of Spatially Oriented Molecules. *Rev. Sci. Instrum.* **2005**, *76*, 123103. [[CrossRef](#)]
10. Thoman, J.W., Jr.; Chandler, D.W.; Parker, D.H.; Janssen, M.H.M. Two-dimensional Imaging of Photofragments. *Laser Chem.* **1988**, *9*, 27–46. [[CrossRef](#)]
11. Rakitzis, T.P.; van den Brom, A.J.; Janssen, M.H.M. Directional Dynamics in the Photodissociation of Oriented Molecules. *Science* **2004**, *303*, 1852–1854. [[CrossRef](#)]
12. Van den Brom, A.J.; Rakitzis, T.P.; Janssen, M.H.M. Molecular frame properties from photodissociation of laboratory-oriented symmetric top and chiral molecules. *Phys. Scr.* **2006**, *73*, C83–C88. [[CrossRef](#)]
13. Blum, K.; Musigmann, M.; Thompson, D. Elastic Electron Collision with Chiral and Oriented Molecules. In *Supercomputing, Collision Processes, and Applications. Physics of Atoms and Molecules*; Bell, K.L., Berrington, K.A., Crothers, D.S.F., Hibbert, A., Taylor, K.T., Eds.; Springer: Boston, MA, USA, 2002. [[CrossRef](#)]
14. Lombardi, A.; Palazzetti, F.; Maciel, G.S.; Aquilanti, V.; Sevryuk, M.B. Simulation of oriented collision dynamics of simple chiral molecules. *Int. J. Quant. Chem.* **2011**, *111*, 1651–1658. [[CrossRef](#)]
15. Rezende, M.V.C.S.; Coutinho, N.D.; Palazzetti, F.; Lombardi, A.; Carvalho-Silva, V.A. Nucleophilic substitution vs elimination reaction of bisulfide ions with substituted methanes: Exploration of chiral selectivity by stereodirectional first-principles dynamics and transition state theory. *J. Mol. Model.* **2019**, *25*, 227. [[CrossRef](#)] [[PubMed](#)]

16. Hashinokuchi, M.; Che, D.-C.; Watanabe, D.; Fukuyama, T.; Koyano, I.; Shimizu, Y.; Woelke, A.; Kasai, T. Single $|J \Omega M_J\rangle$ state-selection of OH radicals using an electrostatic hexapole field. *Phys. Chem. Chem. Phys.* **2003**, *5*, 3911–3915. [[CrossRef](#)]
17. He, L.; Bulthuis, J.; Luo, S.; Wang, J.; Lu, C.; Stolte, S.; Ding, D.; Roeterdink, W.G. Laser induced alignment of state-selected CH₃I. *Phys. Chem. Chem. Phys.* **2015**, *17*, 24121–24128. [[CrossRef](#)]
18. Cho, V.A.; Bernstein, R.B. Tight focusing of beams of polar polyatomic molecules via the electrostatic hexapole lens. *J. Phys. Chem.* **1991**, *95*, 8129–8136. [[CrossRef](#)]
19. Hain, T.D.; Moision, R.M.; Curtiss, T.J. Hexapole state-selection and orientation of asymmetric top molecules: CH₂F₂. *J. Chem. Phys.* **1999**, *111*, 6797. [[CrossRef](#)]
20. Che, D.-C.; Palazzetti, F.; Okuno, Y.; Aquilanti, V.; Kasai, T. Electrostatic Hexapole State-Selection of the Asymmetric-Top Molecule Propylene Oxide. *J. Phys. Chem. A* **2010**, *114*, 3280–3286. [[CrossRef](#)]
21. Palazzetti, F.; Maciel, G.S.; Kanda, K.; Nakamura, M.; Che, D.-C.; Kasai, T.; Aquilanti, V. Control of conformers combining cooling by supersonic expansion of seeded molecular beams with hexapole selection and alignment: Experiment and theory on 2-butanol. *Phys. Chem. Chem. Phys.* **2014**, *16*, 9866–9875. [[CrossRef](#)]
22. Caglioti, C.; Nakamura, M.; Che, D.-C.; Tsai, P.-Y.; Palazzetti, F. Conformer Selection by Electrostatic Hexapoles: A Theoretical Study on 1-Chloroethanol and 2-Chloroethanol. *Symmetry* **2022**, *14*, 317. [[CrossRef](#)]
23. Che, D.-C.; Kanda, K.; Palazzetti, F.; Aquilanti, V.; Kasai, T. Electrostatic hexapole state-selection of the asymmetric-top molecule propylene oxide: Rotational and orientational distributions. *Chem. Phys.* **2012**, *399*, 180–192. [[CrossRef](#)]
24. Nakamura, M.; Yang, S., Jr.; Tsai, P.Y.; Kasai, T.; Che, D.-C.; Lombardi, A.; Palazzetti, F.; Aquilanti, V. Hexapole-Oriented Asymmetric-Top Molecules and Their Stereodirectional Photodissociation Dynamics. *J. Phys. Chem. A* **2016**, *120*, 5389–5398. [[CrossRef](#)]
25. Nakamura, M.; Yang, S.-J.; Lin, K.-C.; Kasai, T.; Che, D.-C.; Lombardi, A.; Palazzetti, F.; Aquilanti, V. Stereodirectional images of molecules oriented by a variable-voltage hexapolar field: Fragmentation channels of 2-bromobutane electronically excited at two photolysis wavelengths. *J. Chem. Phys.* **2017**, *147*, 013917. [[CrossRef](#)]
26. Nakamura, M.; Palazzetti, F.; Tsai, P.-Y.; Yang, S., Jr.; Lin, K.-C.; Kasai, T.; Che, D.-C.; Lombardi, A.; Aquilanti, V. Vectorial imaging of the photodissociation of 2-bromobutane oriented via hexapolar state selection. *Phys. Chem. Chem. Phys.* **2019**, *21*, 14164–14172. [[CrossRef](#)] [[PubMed](#)]
27. Nakamura, M.; Chang, H.-P.; Lin, K.-C.; Kasai, T.; Che, D.-C.; Palazzetti, F.; Aquilanti, V. Stereodynamic Imaging of Bromine Atomic Photofragments Eliminated from 1-Bromo-2-methylbutane Oriented via Hexapole State Selector. *J. Phys. Chem. A* **2019**, *123*, 6635–6644. [[CrossRef](#)] [[PubMed](#)]
28. Chang, H.-P.; Nakamura, M.; Kasai, T.; Lin, K.-C. Photodissociation study of spatially oriented (R)-3-bromocamphor by the hexapole state selector. *Mol. Phys.* **2021**, *120*, e1985643. [[CrossRef](#)]
29. Che, D.-C.; Nakamura, M.; Chang, H.-P.; Lin, K.-C.; Kasai, T.; Aquilanti, V.; Palazzetti, F. UV Photodissociation of Halothane in a Focused Molecular Beam: Space-Speed Slice Imaging of Competitive Bond Breaking into Spin–Orbit-Selected Chlorine and Bromine Atoms. *J. Phys. Chem. A* **2020**, *124*, 5288–5296. [[CrossRef](#)] [[PubMed](#)]
30. Efrati, A.; Irvine, W.T.M. Orientation-Dependent Handedness and Chiral Design. *Phys. Rev. X* **2014**, *4*, 011003. [[CrossRef](#)]
31. Shang, Y.; Wang, Z.; Yang, D.; Wang, D.; Ma, C.; Tao, M.; Sun, K.; Yang, J.; Wang, J. Orientation Ordering and Chiral Superstructures in Fullerene Monolayer on Cd (0001). *Nanomaterials* **2020**, *10*, 1305. [[CrossRef](#)]
32. Gershnabel, E.; Averbukh, I.S. Orienting Asymmetric Molecules by Laser Fields with Twisted Polarization. *Phys. Rev. Lett.* **2018**, *120*, 083204. [[CrossRef](#)] [[PubMed](#)]
33. Milner, A.A.; Fordyce, J.A.M.; MacPhail-Bartley, I.; Wasserman, W.; Milner, V.; Tutunnikov, I.; Averbukh, S. Controlled Enantioselective Orientation of Chiral Molecules with an Optical Centrifuge. *Phys. Rev. Lett.* **2019**, *122*, 223201. [[CrossRef](#)] [[PubMed](#)]
34. Yachmanev, A.; Onvlee, J.; Zak, E.; Owens, A.; Küpper, J. Field-Induced Diastereomers for Chiral Separation. *Phys. Rev. Lett.* **2019**, *123*, 243202. [[CrossRef](#)] [[PubMed](#)]
35. Lee, H.-N.; Chang, L.-C.; Su, T.-M. Optical rotamers of substituted simple alkanes induced by macroscopic translation-rotational motions. *Chem. Phys. Lett.* **2011**, *507*, 63–68. [[CrossRef](#)]
36. Su, T.M.; Palazzetti, F.; Lombardi, A.; Grossi, G. Molecular alignment and chirality in gaseous streams and vortices. *Rend. Fis. Acc. Lincei* **2013**, *24*, 291–297. [[CrossRef](#)]
37. Zare, R.N.; Harter, W.G. *Angular Momentum, Understanding Spatial Aspects in Chemistry and Physics*; Wiley-Interscience: New York, NY, USA, 1988.
38. Orr-Ewing, A.J.; Zare, R.N. Orientation and alignment of reaction products. *Annu. Rev. Phys. Chem.* **1994**, *45*, 315. [[CrossRef](#)]
39. Eppink, A.T.J.B.; Parker, D.H. Velocity map imaging of ions and electrons using electrostatic lenses: Application in photoelectron and photofragment ion imaging of molecular oxygen. *Rev. Sci. Instr.* **1997**, *68*, 3477. [[CrossRef](#)]
40. Gebhardt, C.R.; Rakitzis, T.P.; Samartzis, P.C.; Ladopoulos, V.; Kitsopoulos, T.N. Slice imaging: A new approach to ion imaging and velocity mapping. *Rev. Sci. Instr.* **2001**, *72*, 3848. [[CrossRef](#)]
41. Townsend, D.; Minitti, M.P.; Suits, A.G. Direct current slice imaging. *Rev. Sci. Instr.* **2003**, *74*, 2530. [[CrossRef](#)]
42. Che, D.-C.; Kawamata, H.; Nakamura, M.; Kasai, T.; Lin, K.-C. A vector correlation study using a hexapole-oriented molecular beam: Photodissociation dynamics of oriented isohaloethane. *Phys. Chem. Chem. Phys.* **2022**, *24*, 5914–5920. [[CrossRef](#)] [[PubMed](#)]